

2010

The Trypanosoma *brucei* MitoCarta and its regulation and splicing pattern during development

Xiaobai Zhang
Nanjing University

Juan Cui
University of Georgia, jcui@unl.edu

Daniel Nilsson
University of Bern

Kapila Gunasekera
University of Bern

Astrid Chanfon
University of Bern

See next page for additional authors

Follow this and additional works at: <http://digitalcommons.unl.edu/csearticles>

Zhang, Xiaobai; Cui, Juan; Nilsson, Daniel; Gunasekera, Kapila; Chanfon, Astrid; Song, Xiaofeng; Wang, Huinan; Xu, Ying; and Ochsenteiter, Torsten, "The Trypanosoma *brucei* MitoCarta and its regulation and splicing pattern during development" (2010). CSE Journal Articles. 179.
<http://digitalcommons.unl.edu/csearticles/179>

This Article is brought to you for free and open access by the Computer Science and Engineering, Department of at DigitalCommons@University of Nebraska - Lincoln. It has been accepted for inclusion in CSE Journal Articles by an authorized administrator of DigitalCommons@University of Nebraska - Lincoln.

Authors

Xiaobai Zhang, Juan Cui, Daniel Nilsson, Kapila Gunasekera, Astrid Chanfon, Xiaofeng Song, Huinan Wang, Ying Xu, and Torsten Ochsenreiter

The *Trypanosoma brucei* MitoCarta and its regulation and splicing pattern during development

Xiaobai Zhang^{1,2}, Juan Cui², Daniel Nilsson³, Kapila Gunasekera³, Astrid Chanfon³, Xiaofeng Song¹, Huinan Wang¹, Ying Xu^{2,4,*} and Torsten Ochsenreiter³

¹Department of Biomedical Engineering, Nanjing University of Aeronautics and Astronautics, Nanjing, Jiangsu 210016 China, ²Computational Systems Biology Lab, Department of Biochemistry and Molecular Biology and Institute of Bioinformatics, University of Georgia, Athens, GA 30602, USA, ³Institute of Cell Biology, University of Bern, Switzerland and ⁴College of Computer Science and Technology, Jilin University, Changchun, Jilin 130000 China

Received March 10, 2010; Revised June 22, 2010; Accepted June 25, 2010

ABSTRACT

It has long been known that trypanosomes regulate mitochondrial biogenesis during the life cycle of the parasite; however, the mitochondrial protein inventory (MitoCarta) and its regulation remain unknown. We present a novel computational method for genome-wide prediction of mitochondrial proteins using a support vector machine-based classifier with ~90% prediction accuracy. Using this method, we predicted the mitochondrial localization of 468 proteins with high confidence and have experimentally verified the localization of a subset of these proteins. We then applied a recently developed parallel sequencing technology to determine the expression profiles and the splicing patterns of a total of 1065 predicted MitoCarta transcripts during the development of the parasite, and showed that 435 of the transcripts significantly changed their expressions while 630 remain unchanged in any of the three life stages analyzed. Furthermore, we identified 298 alternatively splicing events, a small subset of which could lead to dual localization of the corresponding proteins.

INTRODUCTION

Trypanosoma brucei, a unicellular, flagellated protozoan parasite, is the causative agent of human African trypanosomiasis and the cattle-wasting disease Nagana in sub-Saharan Africa. *T. brucei* has a digenetic life cycle alternating between the tsetse fly and a mammal host. Besides being a human and veterinary pathogen, it has played a key role in the discovery and understanding of

a number of general biological principles such as RNA editing, antigenic variation, GPI anchoring and *trans*-splicing (1–6). The latter is a mechanism by which *T. brucei* processes the 5'-ends of its polycistronic mRNAs through the addition of a 39 nucleotide leader sequence. A unique aspect of the trypanosome biology is the development and regulation of its single, large mitochondrion. In the insect vector, the parasite has a fully developed organelle containing numerous cristae, electron transport complexes, where energy production is performed through electron transportation coupled with oxidative phosphorylation (7). In contrast, the parasite in bloodstream exclusively uses glycolysis in a specialized organelle, the glycosome, to meet its energy needs [reviewed in (8)]. This is also reflected in the size and the structure of the mitochondrion with a reduced number of cristae and reduced volume (9). As of today, the precise protein composition of the organelle largely remains unknown. However, recently, a comprehensive study identified mitochondrial proteins in insect form *T. brucei* using a shotgun proteomics approach, and assigned 597 proteins to the mitochondrion with high quality (10). In *T. brucei*, only 18 proteins have been predicted to be encoded in its mitochondrial genome (11,12), and thus the vast majority of the identified mitochondrial proteins are nuclear encoded, translated in the cytoplasm, and imported into the mitochondrion. Many proteins that are imported into the mitochondrion have targeting signals, typically at the N-termini (13–17), and in some cases at the C-termini (18) or protein internal (19,20). However, numerous mitochondrial proteins were found to be lacking such signal peptides including proteins that have been shown to be imported into mitochondria in trypanosomes (13,21–23). This poses a major challenge in the identification of mitochondrial proteins.

*To whom correspondence should be addressed. Tel: +1 706 542 9779; Fax: +1 706 542 9751; Email: xyn@bmb.uga.edu

To date, a number of computational methods have been developed to predict mitochondrial proteins. These methods use different protein features, such as amino acid composition [AAC; e.g. MitPred (24), Predotar (25), PSORTII (26), PLOC (27), NNPSL (28)], physicochemical properties [e.g. Predotar (25), Proteome Analyst (29), LOCSVMPSI (30), ESLpred (31), LOCtree (32)], N-terminal signal peptides [e.g. TargetP (33), iPSORT (34), PredSL (35)] and Pfam domain occurrences [e.g. MITOPRED (36,37), MitPred (24)]. They employ different computational techniques, such as support vector machine [SVM; e.g. ELSpred (31), LOCSVMPSI (30), MitPred (24), PLOC (27), SubLoc (38)], artificial neural network [ANN; e.g. Predotar (25), PredSL (35), TargetP (33)], hidden Markov model [HMM; e.g. MitPred (24), PredSL (35)], k-nearest neighbor [k-NN; e.g. PSORTII (26), WoLF PSORT (39,40)] and expert systems [e.g. iPSORT (34), MitoProtII (41)]. While these methods have greatly advanced our knowledge about mitochondrial localization, they have a number of key limitations. For example, the N-terminal signal peptide-based approaches, though very popular, have intrinsic limitations in recognizing mitochondrial outer and inner membrane proteins as well as transmembrane proteins that do not seem to have any apparent targeting peptides. The prediction performance by Pfam domain-based methods, not based on targeting signals, is limited by the reality that there are no detectable Pfam domains that can clearly distinguish mitochondrial from non-mitochondrial proteins (24). One common issue with all these prediction methods is that while some of them can make accurate predictions of several subcellular compartments such as nucleus or cytoplasm, none of them can predict the mitochondrial localization very accurately.

We present a novel computational approach for prediction of mitochondrial proteins in *T. brucei*. By applying this approach, we added 468 new proteins to the pool of mitochondrial proteins. We verified a subset of these proteins using biological and biochemical assays, and then analyzed the regulation of MitoCarta gene expression and splicing patterns using a novel sequencing approach.

MATERIALS AND METHODS

Datasets

Positive data. 597 proteins identified as targeted to mitochondria with high (401) or moderate (196) confidence in a recent proteomic study on *T. brucei* (10) were chosen as our positive dataset. This dataset is available as Supplementary Table S1.

Negative data. 1318 proteins found in subcellular locations of *T. brucei* other than mitochondria in the same study (10) were collected. An additional 1353 potential non-mitochondrial proteins were compiled from the *T. brucei* proteome (9192 proteins from ftp://ftp.sanger.ac.uk/pub/databases/T.brucei_sequences/T.brucei_genome_v4, www.genedb.org) by removing entries either annotated as mitochondrial or as 'hypothetical', 'potential' or 'putative' proteins. Proteins with BLAST sequence similarities to any positive samples or

any potential mitochondrial proteins in the MitoP2 database (E-value cutoff = 0.5) (www.mitop.de:8080/mitop2/) were removed. 1290 non-mitochondrial proteins remained and were selected as our negative set. This dataset is available as Supplementary Table S2.

Training and test sets. an SVM-based classifier requires both training and test sets. The collected positive and negative sets were split by randomly selecting 3/4th of the data from each set as the training sets and the remaining as the test data. To evaluate the accuracy and stability of our trained classifiers, this random sampling process was repeated fifty times, resulting in 50 groups of training and test sets.

Computational method

Protein features. We examined various features of proteins, including those widely used for protein localization prediction, in order to identify a list of features that can distinguish well mitochondrial from non-mitochondrial proteins. The initial features can be grouped into three categories: basic sequence features, physicochemical properties and signal peptide and transmembrane topology. Details are given in Supplementary Table S3.

Support vector machine. SVM has been successfully used to solve a wide range of biological data mining problems (30,42,43), due to its effectiveness to deal with multidimensional datasets with complex relationships among the data elements. In this study, LIBSVM (<http://www.csie.ntu.edu.tw/~cjlin/libsvm>) with the popular non-linear *Gaussian Radial Basis Function kernel* (RBF) (44) was used for our classification.

Feature selection. LIBSVM was used to select discriminative features between the positive and the negative training sets. Given a set of candidate features, an *F*-score is calculated for each feature element to measure its discriminative power between the positive and the negative sets, and for the *i*-th feature, the *F*-score is calculated by

$$F(i) = \frac{(\bar{x}_i^{(+)} - \bar{x}_i)^2 + (\bar{x}_i^{(-)} - \bar{x}_i)^2}{[1/(n_+ - 1)] \sum_{k=1}^{n_+} (x_{k,i}^{(+)} - \bar{x}_i^{(+)})^2 + [1/(n_- - 1)] \sum_{k=1}^{n_-} (x_{k,i}^{(-)} - \bar{x}_i^{(-)})^2}, \quad (1)$$

where \bar{x}_i , $\bar{x}_i^{(+)}$ and $\bar{x}_i^{(-)}$ are the average value of the *i*th feature over the whole, the positive and negative dataset, respectively; $x_{k,i}^{(+)}$ is the *i*-th feature of the *k*-th positive data and $x_{k,i}^{(-)}$ is the *i*-th feature of the *k*-th negative data; n_+ and n_- are the numbers of positive and negative data, respectively. The larger an *F*-score is, the more discriminative power the feature has. As our goal is to use the fewest number of features to achieve the best classification performance, a subset of feature elements with high *F*-score and having the smallest balanced error rate (BER) in 5-fold cross validation are selected:

$$BER = \frac{1}{2} \left(\frac{fn}{tp + fn} + \frac{fp}{tn + fp} \right), \quad (2)$$

Where tp and tn are the numbers of true positives and true negatives, respectively, and fp and fn are the numbers of false positives and false negatives, respectively.

In a final assessment of the discriminative power of each selected feature element, we used the mean and the standard deviation in an analysis of variance (ANOVA) to compare the distributions of the feature between the positive and the negative samples.

Performance evaluation

For each group of training and testing sets, a prediction model is obtained that optimizes its performance on both the training and test data. Four common measures were used to evaluate the performance, namely prediction sensitivity: $Se = tp/(tp + fn)$, prediction specificity: $Sp = tn/(tn + fp)$, prediction accuracy: $Acc = (tp + tn)/(tp + fn + tn + fp)$ and the Matthews correlation coefficient of the predictions: $MCC = (tp \times tn - fp \times fn)/\sqrt{(tp + fp)(tp + fn)(tn + fp)(tn + fn)}$ (45), with $MCC = 1$ representing a perfect prediction and 0 a random prediction. The trained model with the highest MCC is selected as the final prediction model in our study, henceforth referred to as *Trypanosoma* mitochondrial protein predictor (TMPP).

For a given query protein, the following function score (s) was used in TMPP to predict if the protein is mitochondrial:

$$s(x) = \sum_{i=1}^N y_i \alpha_i k(x, x_i) + b, \quad (3)$$

where k is the RBF kernel function that measures the distance between the input vector x and the stored training vector x_i ; $y_i \in \{1, -1\}$ indicates a positive or negative sample for the i -th training vector; α_i is the Lagrange multiplier for the i -th training vector, which is computed by quadratic programming, and b is the threshold for defining the hyperplane. A positive score predicts a mitochondrial protein. To evaluate the reliability of an assigned class, we introduce prediction precision (PP) as follows:

$$PP = \begin{cases} tp/(tp + fp) & \text{if } s > 0 \\ tn/(tn + fn) & \text{if } s \leq 0 \end{cases} \quad (4)$$

Based on the prediction on 597 positive and 1290 negative proteins, we define three levels of prediction confidence, namely *high* when $PP > 0.9$, *medium* when $0.8 \leq PP < 0.9$ and *low* when $PP \leq 0.8$.

Cell lines and localization

T. brucei brucei AnTat 1.1 and MITat 1.2 (221) were used for the expression and splicing profile study. Late procyclic forms of AnTat 1.1 were cultivated in SDM79 supplemented with 10% FBS. For short stumpy bloodstream forms of AnTat 1.1, mice were immunosuppressed with 260 mg kg^{-1} cyclophosphamide (Sigma) 24 hours prior to intraperitoneal injection of 10^6 parasites. Short stumpy parasites were harvested 5 days post-infection at a density of $2-4 \times 10^8$ cells ml^{-1} blood. 75–80% of the cells showed a

short stumpy phenotype as determined by light microscopy of blood smears after methanol fixation. Long slender forms were harvested from untreated mice at day three post-infection at a density of $<5 \times 10^7$ cells ml^{-1} blood.

Genes were amplified by PCR from genomic DNA of *T. brucei* Mitat 1.2. Procyclic cells of *T. brucei* Mitat 1.2 were grown in semi-defined medium (SDM-79) supplemented with 10% fetal bovine serum to a density of 5×10^6 cells ml^{-1} . For the localization study, cells were transiently transformed with 20 μg of plasmid pG-EGFP β - Δ LII containing the gene of interest with a C-terminal green fluorescent protein tag as described in (46). For fluorescence microscopy, cells were stained with Mitotracker for 15 min at 37°C subsequently washed in PBS pH 7, and then fixed first for 1 min with 1% Paraformaldehyde and then for 5 min in ice cold methanol on a microscopic slide. For Western blotting, 10^7 cells were fractionated using a detergent lysis procedure followed by differential centrifugation steps as described in (47). Fractions were probed with polyclonal HSP70 antibody (kind gift from J. Bangs of Madison, Wisconsin), monoclonal iron sulfur protein antibody (kind gift from S.L. Hajduk, University of Georgia) and anti-GFP (Invitrogen).

PCR and cloning

PCR was done using the gene specific oligonucleotides and genomic DNA from *T. brucei* Mitat 1.2 in 25 μl (1 unit PFU Polymerase (NEB, USA), 2.5 μl 10 \times buffer (NEB, USA), 2 mM $MgCl_2$, 400 μM dNTPs, 30 ng $gDNA$). After restriction digest 200 ng of each the PCR product and the vector pG-EGFP β - Δ LII were ligated in 20 μl using T4 DNA ligase (NEB, USA) at 14°C overnight.

RNA extraction, library construction and sequencing

First strand cDNA was synthesized from polyA RNA using random hexamers and Superscript II reverse transcriptase. Adapters were ligated to the purified cDNA using a customized bar-coded paired-end Illumina adapter (Fasteris, Geneva, Switzerland). After purification, each cDNA library was amplified using the standard Illumina mRNA-SEQ library amplification protocol. Fragments in the range 120–160 bp were gel purified and sequencing on the Illumina Genome Analyzer was carried out using the following sequencing primer (spliced leader primer 5'-ACCGAGATCTACAGT TTCTGTACTATATTG-3').

Base calling was performed using the Genome Analyzer Pipeline (Illumina). Sequence reads of at least 24 nt were separated according to identified barcodes. The reads were mapped to the genome sequence of *T. brucei* TREU927 using maq (48) (<http://maq.sourceforge.net>) with $n = 3$ and an effective first read length of 24. Tag counts were normalized to the library size and scaled linearly to reflect counts of tags per million (TPM). Mapped tags were assigned to the downstream annotated protein-encoding gene. Tags mapping internally to a coding sequence (CDS) were assigned to it as internal splice sites. Alternatively, spliced leader addition sites were cataloged for each gene. Genes with $\leq 60\%$ tags in the assigned

major splice site were designated alternatively spliced. Differences in expression levels of a gene in two different libraries were tested for significance according to Audic and Claverie with a threshold of $P < 10^{-5}$ (49). A test for statistically significant difference (Fisher two-tailed test, $P < 10^{-5}$) between the normalized counts of sites was made for genes with different major splice sites in two life cycle stages. Significant differences were termed differential *trans*-splicing events. Expression levels were visualized as heatmaps after \log_2 transformation and hierarchical average linkage clustering of Euclidean distances using MeV (50) (<http://www.tm4.org/mev.html>).

RESULTS AND DISCUSSION

Features selected for distinguishing mitochondrial proteins

In order to identify a list of features that can well distinguish mitochondrial from non-mitochondrial proteins, we have examined 18 protein features, represented as 605 feature elements for each protein sequence (see Supplementary Table S3). From the original list of 605 feature elements, 66 discriminative feature elements were extracted by feature selection algorithm in LIBSVM. Details are given in Supplementary Table S4.

Basic sequence attributes. Mitochondrial proteins tend to have targeting signals in their N-termini, which may have a distinctive AAC. Hence, we decided to consider the AAC of the N-terminal residues and the remaining residues separately. We examined the conventional AAC and different types of split-AAC, which is calculated for the first n N-terminal residues for $n = 15, 20, 25, 30, 35$, respectively, and the remaining residues separately, by estimating the distinguishing power of these feature vectors through SVM based on 5-fold cross validation. Di-amino acid composition is also considered in our study. As shown in Supplementary Table S5, the conventional AAC gave the worst accuracy, while the split-AAC with $n = 30$ gave the best result and showed strong biases between mitochondrial proteins and non-mitochondrial proteins. As shown in Supplementary Figure S1, AAC in the first 30 N-terminal residues differs substantially from that in the remaining residues of mitochondrial proteins, while the difference is not nearly as remarkable as in non-mitochondrial proteins. Specifically, the N-terminal residues of mitochondrial proteins are rich in positively charged residue, arginine, while poor in negatively charged residues, aspartic acid and glutamic acid, reconfirming the discovery made in previous studies in trypanosomes and other systems (34,35,51). We also observed that the N-terminal mitochondrial sequences have more phenylalanine and tryptophan, but less lysine and in the remaining residues mitochondrial proteins have relatively high percentages of aromatic residues, namely histidine, tryptophan and tyrosine, but lower of hydrophilic residues, i.e. cysteine and asparagine, compared to non-mitochondrial proteins. All the aforementioned discriminative features were successfully selected by the feature selection program (Supplementary Table S4).

Physicochemical properties. Dubchak and coworkers have developed three general descriptors: *composition*,

transition and *distribution*, to measure various structural and physicochemical properties of proteins, such as hydrophobicity, Van der Waals volume, polarity, polarizability, charge, secondary structure and solvent accessibility (52). We have adopted the three descriptors to represent these properties in our feature selection. In addition, we have also considered some structural properties such as secondary structural content (53,54), estimated radius of gyration (55), unfoldability (56) and disordered regions (56) of candidate proteins, considering the potential relevance of these properties to identification of mitochondrial proteins. Some physicochemical properties, namely normalized Van der Waals volume, polarity, polarizability, charge and solvent accessibility, showed strong biases to mitochondrial proteins compared to the non-mitochondrial proteins. Details are given in Supplementary Table S4.

Signal peptide and transmembrane topology. Signal peptides are important for targeting proteins from the cytosol to the endoplasmic reticulum (ER) membrane and for subsequent transport through the secretory pathways (57,58). Both alpha-helical and beta-barrel trans-membrane regions were considered. Our analysis revealed that signal peptides and trans-membrane regions, particularly beta-barrel trans-membrane regions are present less frequently in mitochondrial proteins than in non-mitochondrial proteins. A similar observation is made in other organisms, including yeast, mouse and human. Detailed results are given in Supplementary Table S6.

Evaluation of prediction performance

Training and test. The prediction performance of our trained SVM-based classifier was stable across all 50 test sets, on which the MCC ranges from 0.656 to 0.752, and both sensitivity and specificity are above 80%, as detailed in Table 1, strongly suggesting the effectiveness and stability of our trained classifiers.

Prediction reliability. To evaluate the reliability of the predicted mitochondrial proteins, we have analyzed the relationship between the output score (s) and the prediction precision (PP). As shown in Figure 1, a prediction score higher than 0.8 indicates a mitochondrial protein with high confidence ($PP > 0.9$), a score lower than 0.8 but not lower than 0.4 indicates a mitochondrial protein with medium confidence ($0.8 \leq PP < 0.9$) and a positive score lower than 0.4 assigns a protein to mitochondrial with low confidence ($PP \leq 0.8$).

Our prediction program correctly predicted 535 mitochondrial and 1238 non-mitochondrial proteins among the 597 positive and 1290 negative samples, respectively. Of the 535 predicted mitochondrial proteins, 82% are

Table 1. Prediction performance on 50 testing sets

	MCC	Se	Sp	Acc
Best performance	0.752	0.823	0.926	0.894
Worst performance	0.656	0.801	0.874	0.852
Mean	0.709	0.816	0.901	0.875
Std	0.029	0.014	0.018	0.014

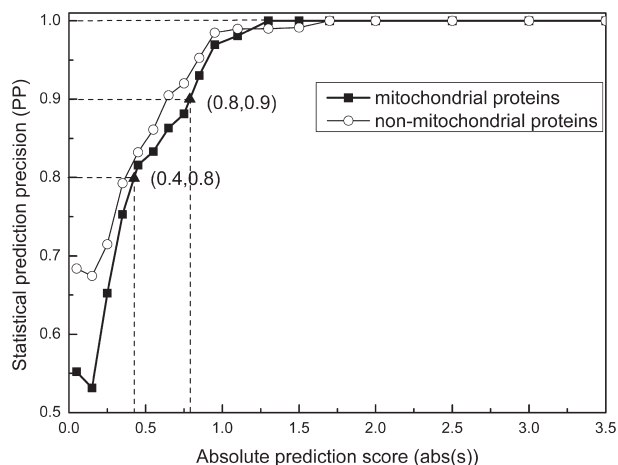


Figure 1. Statistical relationship between the prediction accuracy and the SVM score. The relationship is based on the analysis of 597 (positive set) and 1290 (negative set). The *x*-axis is the absolute SVM score and the *y*-axis represents prediction precision.

Table 2. Comparison of prediction performance of 14 methods applied on 147 mitochondrial and 325 non-mitochondrial proteins

Method	MCC	Se	Sp	Acc
TMPP	0.752	0.823	0.926	0.894
WoLF PSORT	0.577	0.605	0.926	0.826
Predotar	0.543	0.612	0.901	0.811
MitoProt	0.539	0.735	0.821	0.794
PredSL	0.532	0.558	0.923	0.809
PSORT	0.474	0.497	0.920	0.788
TargetP	0.459	0.442	0.938	0.784
Mitpred	0.439	0.469	0.914	0.775
MITOPRED	0.422	0.667	0.772	0.739
iSPORT	0.419	0.497	0.886	0.765
Proteome Analyst	0.383	0.231	0.990	0.754
ELSpred	0.356	0.476	0.855	0.737
PLOC	0.320	0.429	0.862	0.727
SubLoc	0.243	0.517	0.732	0.665

predicted with high confidence, while 11% and 7% are predicted with medium and low confidence, respectively.

Comparison with other methods. The performance of program TMPP has been compared with publicly available programs (see Supplementary Table S7), including MitPred (24), Predotar v1.03 (25), PSORTII (26), PLOC (27), Proteome Analyst (29), ESLpred (31), TargetP v1.1 (33), iSPORT (34), PredSL (35), MITOPRED (36,37), SubLoc v1.0 (38), WoLF PSORT (39,40) and MitoProtII (41). All these programs have been applied to the same test set containing 147 mitochondrial and 325 non-mitochondrial proteins. The prediction results of these programs are summarized in Table 2. TMPP outperforms all the other programs in terms of both the overall prediction accuracy and MCC on the independent test set. Currently MCC is considered to be the most reliable and robust criterion for assessing trained classifiers (24,36).

A common limitation among the N-terminal information-based methods is that a significant number

of mitochondrial proteins do not have targeting signals at N terminus (23,59). TMPP outperforms the existing prediction methods through utilizing more features, as well as through better treatment of previously used features such as the AAC in the N terminal regions (see Supplementary Table S5 and Figure S1). TMPP was specifically trained for trypanosome sequences and may have learned domain knowledge that could lead to an advantage over other methods, potentially at the expense of generality.

Prediction of mitochondrial proteins in *T. brucei*

We have applied TMPP to *T. brucei* proteome and assigned 1065 proteins to mitochondrion with PP > 0.9, including 597 proteins previously shown to be associated with the mitochondrion and 468 proteins without any previous mitochondrial association, covering 12% of the whole proteome of *T. brucei*. Similar numbers have been found for the yeast (876), and mouse (1098) MitoCarta, respectively (60,61). Using a reciprocal best BLAST hit approach we identified 137 homologs of the *T. brucei* MitoCarta in the human MitoCarta, 47 of which are disease associated, indicating the potential usefulness of *T. brucei* in studying human disease genes (Supplementary Table S8). When we compared the *T. brucei* to the yeast MitoCarta, we identified 120 homologs mostly in metabolism (33), protein synthesis (14) and iron sulfur cluster assembly (10).

Experimental validation of predicted mitochondrial proteins in *T. brucei*

In order to verify the prediction accuracy we experimentally localized a subset of proteins in the procyclic *T. brucei* cells by immunofluorescence microscopy and Western blotting (Figure 2). Using a C-terminal green fluorescent protein tag, we showed that 9 out of 12 randomly selected proteins from our prediction co-localized with the mitochondrion specific dye Mitotracker (Invitrogen, USA), while two proteins mainly localized to a structure surrounding the nucleus resembling the ER (Supplementary Figure S2). For one protein, we were unable to detect any GFP signal, likely due to very low expression or rapid degradation of the protein. Between the nine mitochondrially localized proteins, we could distinguish two localization patterns. The majority showed an even distribution of the GFP signal throughout the mitochondrial structure (Figure 2), while two proteins had a more punctuated localization (Figure 2, Tb09.160.3050/Tb09.211.3170) similar to the recently described gRNA associated proteins GAP1 and GAP2 (62). In our cases, the GFP signal could reflect the true localization or be due to the overexpression and C-terminal tagging of the protein. We also used an established biochemical assay of detergent lysis followed by differential centrifugation steps SDS-PAGE and western blotting in order to verify the localization (47). Using an antibody to GFP, we detected the majority of the tagged protein in the mitochondrial fraction, which was verified using antibodies to known mitochondrial (Rieske iron-sulfur protein, anti-ISP) and cytosolic (Heat shock

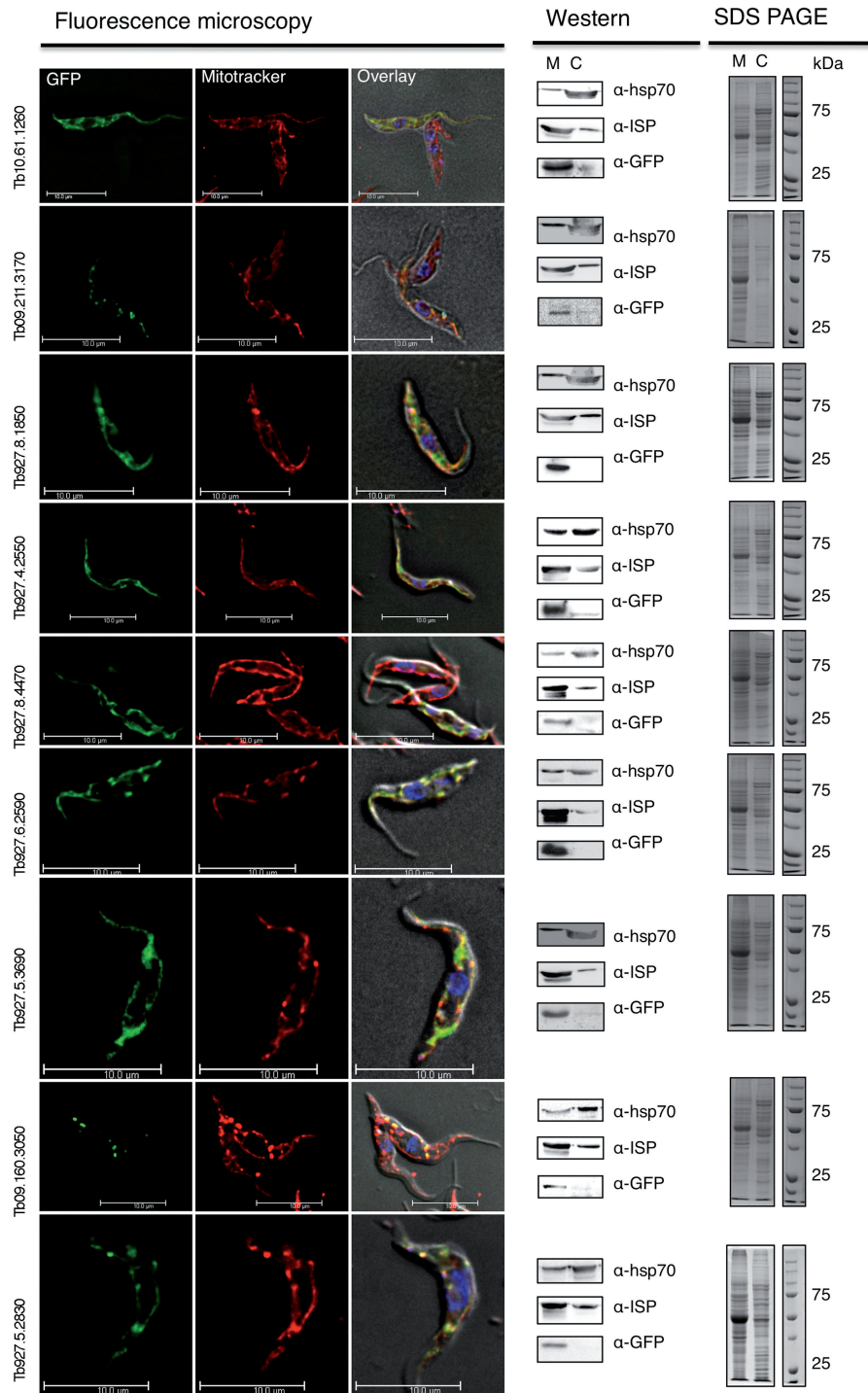


Figure 2. Localization of predicted MitoCarta proteins. The fluorescence microscopy images from nine GFP tagged proteins that were randomly picked from our prediction are shown. First column GFP, second column Mitotracker, third column, overlay including the DAPI and differential interference contrast image, fourth column western blots of total cell protein fractionated in a mitochondrial fraction (M) and a cytosolic fraction (C) and probed with antibodies against the cytosolic HSP70, the mitochondrial iron sulfur protein and GFP, fifth column the SDS-PAGE from the fractionated protein extract.

protein 70, anti-HSP70) proteins (Figure 2). In all cases, the biochemical assay supported the localization detected by immunofluorescence microscopy verifying that the localization is not limited to the individual cells analyzed by microscopy.

The localization of two proteins predicted to be mitochondrial to an ER like structure suggested that there could be a common feature in the localization between the two compartments. Also, since we have investigated only the procyclic form of the parasite, there remains the

possibility of mitochondrial localization of the proteins in other life cycle stages of the parasite. Overall, the mitochondrial localization of 75% of the randomly selected proteins from our prediction supports the strong performance of the presented prediction approach, especially since we have only analyzed one life cycle stage of the parasite.

Regulation of the MitoCarta genes during development

We have recently developed a new method to simultaneously map the 5'-splice sites and the expression profile of *T. brucei* that we named *spliced leader trapping* (SLT) (63). SLT uses the fact that trypanosomes employ *trans-splicing* of a leader sequence onto the 5'-UTR of every mRNA. It allowed us to sequence a short stretch of the 5'-UTR immediate downstream of the spliced leader acceptor site using high throughput parallel sequencing. We obtained more than 4 million sequence tags from the proliferative long slender bloodstream form, the insect form of the parasite as well as from the quiescent short stumpy form. Using this information we were able to monitor the expression profiles of processed mRNAs and the corresponding splicing patterns. We detected transcripts for $\geq 95\%$ of the 1065 MitoCarta genes that had a mean number of 75–87 TPM depending on the stage of the life cycle (Table 3). The number of expressed MitoCarta genes was ~ 1000 independent of the life cycle stage of the parasite (Table 3), which is rather surprising given the large changes in morphology and function of the mitochondrion during development. Of the expressed genes, 630 transcripts did not significantly change in abundance while 435 showed a significant change in expression levels in at least one of the three life cycle stages (Supplementary Table S9). From this data, it appears that $\sim 60\%$ of the MitoCarta is a core set for the mitochondrial biogenesis, while $\sim 40\%$ are life cycle stage specific. However, a significant number of genes thought to be associated with insect form specific physiology are also expressed in the bloodstream form, suggesting that

they are not regulated at the level of transcription but rather at the level of translation and protein stability, as shown for cytochrome c reductase (64). Alternatively, expressions of these transcripts could also indicate novel or previously undetected functions in the bloodstream form mitochondrion. One of the most prominent examples was the succinyl Co-A ligase beta subunit, which is one of the most highly expressed transcripts in cells of the bloodstream form (4344 TPM). Using RNAi, we showed that the loss of transcripts is not only lethal in the insect form of the parasite as had been shown previously but also in the bloodstream form, indicating that the corresponding protein performs an unknown function in the bloodstream form mitochondrion [(65), Supplementary Figure S3].

Splicing

The analysis of our SLT data revealed 298 alternative splicing events in the MitoCarta transcriptome (Supplementary Table S10). We called a transcript alternatively spliced if the major splice site contained less than 60% of the sequence tags. For 51–55 transcripts, depending on the life-cycle stage, the splicing occurred downstream of the annotated AUG start codon potentially leading to a loss or gain of mitochondrial targeting sequences as predicted by TargetP [(33), Figure 3, Supplementary Table S11]. We also detected 23 splicing events that would allow for an N-terminal extension of the encoded protein depending on the splice variant. Five of these transcripts were alternatively spliced such that different splicing events could lead to a change in localization of the corresponding protein products (Supplementary Table S11), which has previously been observed for alternative splice variants of A-kinase anchoring protein 1 in mouse fibroblasts (66). Interestingly, the N-terminal extensions could also lead to a change in localization from mitochondrial to non-mitochondrial by masking the targeting signal through the addition of amino acids to the N-terminus.

Table 3. Expression and splicing profile of the MitoCarta in long slender, short stumpy and procyclic form *T. brucei*

	Long slender (LS)	Short stumpy (SS)	Procyclic (PC)	Total
MitoCarta genes	–	–	–	1065
Differentially regulated	109 (LS to SS)	357 (SS to PC)	350 (LS to PC)	435 ^a
Unchanged expression	–	–	–	630
Alternatively spliced	174	186	154	298 ^b
Differentially spliced	11 (LS to SS)	50 (SS/PC)	45 (LS to PC)	–
Major internal sites	88	90	74	–
Only internal sites	55	51	52	–
N-terminal extensions ^c	–	–	–	23
Genes expressed	934	932	945	–
TPM (mean)	75	81	87	–
TPM (median)	24	22	29	–

^aTotal number of genes that significantly change expression levels.

^bThe major splice site contains less than 60% of the tags.

^cSplice site would allow for N-terminal extension of the reading frame.

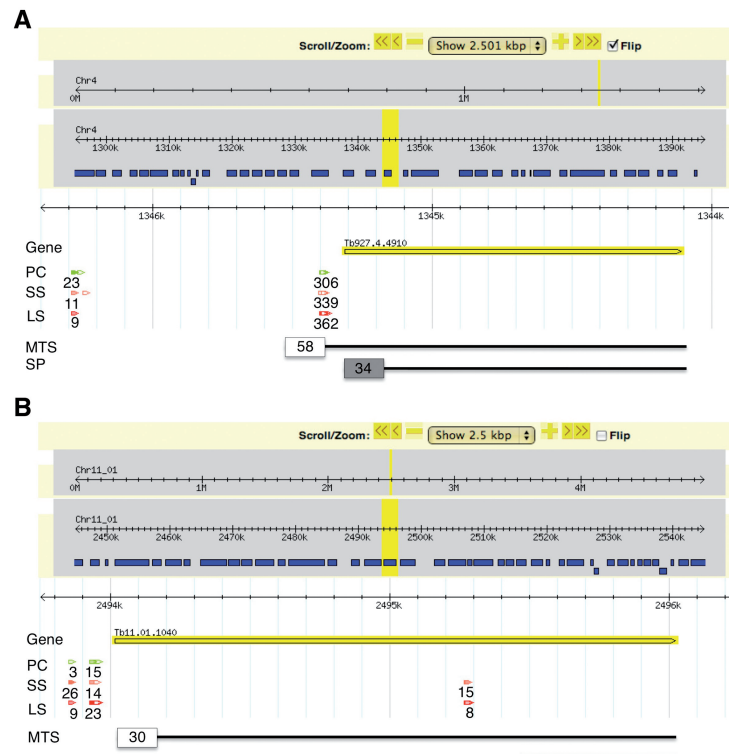


Figure 3. Two examples of alternative splice variants potentially leading to changes in localization. Screenshot of a region from chromosome of 2.5kbp of two genes with SLT data in TPM from procyclic (green), bloodstream long slender (red), short stumpy forms (orange) and potential mitochondrial targeting signals (MTS, white box) and signal peptide sequence (SP, grey box) on the corresponding protein sequences (black line). (A) Tb927.4.4910, the upstream splice site potentially lead to a N-terminal extension of the open reading frame now containing a MTS of 58 amino acids as predicted by MITOPROT (confidence 0.75). The downstream splice site excludes the MTS, instead leading to a SP of 34 amino acids (confidence 0.98, SignalP). (B) Tb11.01.1040, the upstream splice site would allow translation from the currently annotated AUG leading to a protein containing a 30 amino acid MTS (confidence 0.99, MITOPROT), while the downstream, internal splice site would exclude the MTS leading to a 345 amino acid protein.

CONCLUSION

We have identified 66 feature elements to distinguish mitochondrial from non-mitochondrial proteins, and developed an SVM-based classifier to predict mitochondrial proteins in *T. brucei*. Using this approach we predicted the *T. brucei* MitoCarta to contain 1065 proteins, 468 of which did not have assigned cellular components. Using cell biology and biochemical methods, we have verified the localization of 75% of a randomly chosen subset of the predicted proteins supporting the performance of the prediction approach. The regulation of the total mitochondrial proteome indicates a minimal subset of proteins that have to be present to maintain the mitochondrial organelle and the alternative splicing patterns of a subset of MitoCarta transcripts indicate the dual use of the corresponding proteins in other parts of the cell.

SUPPLEMENTARY DATA

Supplementary Data are available at NAR Online.

ACKNOWLEDGEMENTS

The authors thank Drs V. Oltman, F. Zhou and Y. Ou at University of Georgia for inspiring discussions, and would like to acknowledge Isabel Roditi at University of Bern for

providing RNA and critically reading the manuscript. This study was supported in part by computer clusters provided by the University of Georgia Research Computing Center, a partnership between the Office of the Vice President for Research and the Office of the Chief Information Officer.

FUNDING

National Science Foundation (DEB-0830024 and DBI-0542119 to J.C. and Y.X., partial); China Scholarship Council Postgraduate Scholarship Program (to X.B.Z., partial); Swiss National Science foundation (31003A_125194 to T.O., K.G., A.C. and D.N.). Funding for open access charge: National Science Foundation (DEB-0830024).

Conflict of interest statement. None declared.

REFERENCES

- Benne, R., Van den Burg, J., Brakenhoff, J.P., Sloof, P., Van Boom, J.H. and Tromp, M.C. (1986) Major transcript of the frameshifted coxII gene from trypanosome mitochondria contains four nucleotides that are not encoded in the DNA. *Cell*, **46**, 819–826.

2. Horvath, A., Berry, E.A. and Maslov, D.A. (2000) Translation of the edited mRNA for cytochrome b in trypanosome mitochondria. *Science*, **287**, 1639–1640.
3. Borst, P. and Cross, G.A. (1982) Molecular basis for trypanosome antigenic variation. *Cell*, **29**, 291–303.
4. Ferguson, M.A. and Cross, G.A. (1984) Myristylation of the membrane form of a Trypanosoma brucei variant surface glycoprotein. *J. Biol. Chem.*, **259**, 3011–3015.
5. de Almeida, M.L., Turner, M.J., Stambuk, B.B. and Schenkman, S. (1988) Identification of an acid-lipase in human serum which is capable of solubilizing glycosphatidylinositol-anchored proteins. *Biochem. Biophys. Res. Commun.*, **150**, 476–482.
6. Sutton, R.E. and Boothroyd, J.C. (1986) Evidence for trans splicing in trypanosomes. *Cell*, **47**, 527–535.
7. Besteiro, S., Barrett, M.P., Riviere, L. and Bringaud, F. (2005) Energy generation in insect stages of Trypanosoma brucei: metabolism in flux. *Trends Parasitol.*, **21**, 185–191.
8. Michels, P., Bringaud, F., Herman, M. and Hannaert, V. (2006) Metabolic functions of glycosomes in trypanosomatids. *BBA-Molecular Cell Res.*, **1763**, 1463–1477.
9. Vickerman, K. (1965) Polymorphism and mitochondrial activity in sleeping sickness trypanosomes. *Nature*, **208**, 762–766.
10. Panigrahi, A.K., Ogata, Y., Zikova, A., Anupama, A., Dalley, R.A., Acestor, N., Myler, P.J. and Stuart, K.D. (2009) A comprehensive analysis of Trypanosoma brucei mitochondrial proteome. *Proteomics*, **9**, 434–450.
11. Sloof, P., de Haan, A., Eier, W., van Iersel, M., Boel, E., van Steeg, H. and Benne, R. (1992) The nucleotide sequence of the variable region in Trypanosoma brucei completes the sequence analysis of the maxicircle component of mitochondrial kinetoplast DNA. *Mol. Biochem. Parasitol.*, **56**, 289–299.
12. Simpson, L. (1987) The mitochondrial genome of kinetoplastid protozoa: genomic organization, transcription, replication, and evolution. *Annu. Rev. Microbiol.*, **41**, 363–382.
13. Herrmann, J. and Neupert, W. (2000) Protein transport into mitochondria. *Curr. Opin. Microbiol.*, **3**, 210–214.
14. Bertrand, K.I. and Hajduk, S.L. (2000) Import of a constitutively expressed protein into mitochondria from procyclic and bloodstream forms of Trypanosoma brucei. *Mol. Biochem. Parasitol.*, **106**, 249–260.
15. Long, S., Jirku, M., Ayala, F.J. and Lukes, J. (2008) Mitochondrial localization of human frataxin is necessary but processing is not for rescuing frataxin deficiency in Trypanosoma brucei. *Proc. Natl Acad. Sci. USA*, **105**, 13468–13473.
16. Tetaud, E., Giroud, C., Prescott, A.R., Parkin, D.W., Baltz, D., Biteau, N., Baltz, T. and Fairlamb, A.H. (2001) Molecular characterisation of mitochondrial and cytosolic trypanothione-dependent trypanodioxin peroxidases in Trypanosoma brucei. *Mol. Biochem. Parasitol.*, **116**, 171–183.
17. Brown, B.S., Stanislawski, A., Perry, Q.L. and Williams, N. (2001) Cloning and characterization of the subunits comprising the catalytic core of the Trypanosoma brucei mitochondrial ATP synthase. *Mol. Biochem. Parasitol.*, **113**, 289–301.
18. Lee, C., Sedman, J., Neupert, W. and Stuart, R. (1999) The DNA helicase, Hmi1p, is transported into mitochondria by a C-terminal cleavable targeting signal. *J. Biol. Chem.*, **274**, 20937–20942.
19. Folsch, H., Guiard, B., Neupert, W. and Stuart, R.A. (1996) Internal targeting signal of the BCS1 protein: a novel mechanism of import into mitochondria. *EMBO J.*, **15**, 479–487.
20. Chaudhuri, M. and Nargang, F.E. (2003) Import and assembly of Neurospora crassa Tom40 into mitochondria of Trypanosoma brucei in vivo. *Curr. Genet.*, **44**, 85–94.
21. Priest, J.W. and Hajduk, S.L. (2003) Trypanosoma brucei cytochrome c1 is imported into mitochondria along an unusual pathway. *J. Biol. Chem.*, **278**, 15084–15094.
22. Priest, J.W., Wood, Z.A. and Hajduk, S.L. (1993) Cytochromes c1 of kinetoplastid protozoa lack mitochondrial targeting presequences. *Biochim. Biophys. Acta*, **1144**, 229–231.
23. Tasker, M., Timms, M., Hendriks, E. and Matthews, K. (2001) Cytochrome oxidase subunit VI of Trypanosoma brucei is imported without a cleaved presequence and is developmentally regulated at both RNA and protein levels. *Mol. Microbiol.*, **39**, 272–285.
24. Kumar, M., Verma, R. and Raghava, G. (2006) Prediction of mitochondrial proteins using support vector machine and hidden Markov model. *J. Biol. Chem.*, **281**, 5357–5363.
25. Small, I., Peeters, N., Legeai, F. and Lurin, C. (2004) Predotar: A tool for rapidly screening proteomes for N-terminal targeting sequences. *Proteomics*, **4**, 1581–1590.
26. Nakai, K. and Horton, P. (1999) PSORT: a program for detecting sorting signals in proteins and predicting their subcellular localization. *Trends Biochem. Sci.*, **24**, 34–35.
27. Park, K. and Kanehisa, M. (2003) Prediction of protein subcellular locations by support vector machines using compositions of amino acids and amino acid pairs. *Bioinformatics*, **19**, 1656–1663.
28. Reinhardt, A. and Hubbard, T. (1998) Using neural networks for prediction of the subcellular location of proteins. *Nucleic Acids Res.*, **26**, 2230–2236.
29. Lu, Z., Szafron, D., Greiner, R., Lu, P., Wishart, D., Poulin, B., Anvik, J., Macdonell, C. and Eisner, R. (2004) Predicting subcellular localization of proteins using machine-learned classifiers. *Bioinformatics*, **20**, 547–556.
30. Xie, D., Li, A., Wang, M., Fan, Z. and Feng, H. (2005) LOCSVMPSI: a web server for subcellular localization of eukaryotic proteins using SVM and profile of PSI-BLAST. *Nucleic Acids Res.*, **33**, W105.
31. Bhasin, M. and Raghava, G. (2004) ESLpred: SVM-based method for subcellular localization of eukaryotic proteins using dipeptide composition and PSI-BLAST. *Nucleic Acids Res.*, **32**, W414.
32. Nair, R. and Rost, B. (2005) Mimicking cellular sorting improves prediction of subcellular localization. *J. Mol. Biol.*, **348**, 85–100.
33. Emanuelsson, O., Nielsen, H., Brunak, S. and von Heijne, G. (2000) Predicting subcellular localization of proteins based on their N-terminal amino acid sequence. *J. Mol. Biol.*, **300**, 1005–1016.
34. Bannai, H., Tamada, Y., Maruyama, O., Nakai, K. and Miyano, S. (2002) Extensive feature detection of N-terminal protein sorting signals. *Bioinformatics*, **18**, 298–305.
35. Petsalaki, E., Bagos, P., Litou, Z. and Hamodrakas, S. (2006) PredSL: a tool for the N-terminal sequence-based prediction of protein subcellular localization. *Genom., Proteom. Bioinform.*, **4**, 48–55.
36. Guda, C., Fahy, E. and Subramaniam, S. (2004) MITOPRED: a genome-scale method for prediction of nucleus-encoded mitochondrial proteins. *Bioinformatics*, **20**, 1785–1794.
37. Guda, C., Guda, P., Fahy, E. and Subramaniam, S. (2004) MITOPRED: a web server for the prediction of mitochondrial proteins. *Nucleic Acids Res.*, **32**, W372.
38. Hua, S. and Sun, Z. (2001) Support vector machine approach for protein subcellular localization prediction. *Bioinformatics*, **17**, 721–728.
39. Horton, P., Park, K., Obayashi, T., Fujita, N., Harada, H., Adams-Collier, C. and Nakai, K. (2007) WoLF PSORT: protein localization predictor. *Nucleic Acids Res.*, **35**, W585.
40. Horton, P., Park, K., Obayashi, T. and Nakai, K. (2006) Protein subcellular localization prediction with WoLF PSORT. *Proceedings of the 4th Annual Asia Pacific Bioinformatics Conference APBC06*. Taipei, Taiwan, pp. 39–48.
41. Claros, M. and Vincens, P. (1996) Computational method to predict mitochondrially imported proteins and their targeting sequences. *Eur. J. Biochem.*, **241**, 779–786.
42. Cui, J., Liu, Q., Puett, D. and Xu, Y. (2008) Computational prediction of human proteins that can be secreted into the bloodstream. *Bioinformatics*, **24**, 2370–2375.
43. Guo, Y., Yu, L., Wen, Z. and Li, M. (2008) Using support vector machine combined with auto covariance to predict protein-protein interactions from protein sequences. *Nucleic Acids Res.*, **36**, 3025–3030.
44. Burges, C. (1998) A tutorial on support vector machines for pattern recognition. *Data mining knowledge discovery*, **2**, 121–167.
45. Matthews, B. (1975) Comparison of the predicted and observed secondary structure of T4 phage lysozyme. *Biochimica et Biophys. Acta*, **405**, 442–451.

46. Vassella,E., Acosta-Serrano,A., Studer,E., Lee,S., Englund,P. and Roditi,I. (2001) Multiple procyclin isoforms are expressed differentially during the development of insect forms of *Trypanosoma brucei*. *J. Mol. Biol.*, **312**, 597–607.
47. Pusnik,M., Small,I., Read,L.K., Fabbro,T. and Schneider,A. (2007) Pentatricopeptide repeat proteins in *Trypanosoma brucei* function in mitochondrial ribosomes. *Mol. Cell. Biol.*, **27**, 6876–6888.
48. Li,H., Ruan,J. and Durbin,R. (2008) Mapping short DNA sequencing reads and calling variants using mapping quality scores. *Genome Res.*, **18**, 1851–1858.
49. Audic,S. and Claverie,J. (1997) The significance of digital gene expression profiles. *Genome Res.*, **7**, 986–995.
50. Kanehisa,M. and Goto,S. (2000) KEGG: Kyoto encyclopedia of genes and genomes. *Nucleic Acids Res.*, **28**, 27–30.
51. Uboldi,A.D., Lueder,F.B., Walsh,P., Spurck,T., McFadden,G.I., Curtis,J., Likic,V.A., Perugini,M.A., Barson,M., Lithgow,T. *et al.* (2006) A mitochondrial protein affects cell morphology, mitochondrial segregation and virulence in *Leishmania*. *Int. J. Parasitol.*, **36**, 1499–1514.
52. Dubchak,I., Muchnik,I., Holbrook,S. and Kim,S. (1995) Prediction of protein folding class using global description of amino acid sequence. *Proc. Natl Acad. Sci. USA*, **92**, 8700–8704.
53. Eisenhaber,F., Imperiale,F., Argos,P. and Frimmel,C. (1996) Prediction of secondary structural content of proteins from their amino acid composition alone. I. New analytic vector decomposition methods. *Proteins*, **25**, 157–168.
54. Eisenhaber,F., Frimmel,C. and Argos,P. (1996) Prediction of secondary structural content of proteins from their amino acid composition alone. II. The paradox with secondary structural class. *Proteins*, **25**, 169–179.
55. Sabatini,R. and Hajduk,S. (1995) RNA ligase and its involvement in guide RNA/mRNA chimera formation. Evidence for a cleavage-ligation mechanism of *Trypanosoma brucei* mRNA editing. *J. Biol. Chem.*, **270**, 7233–7240.
56. Prilusky,J., Felder,C.E., Zeev-Ben-Mordehai,T., Rydberg,E.H., Man,O., Beckmann,J.S., Silman,I. and Sussman,J.L. (2005) FoldIndex: a simple tool to predict whether a given protein sequence is intrinsically unfolded. *Bioinformatics*, **21**, 3435–3438.
57. von Heijne,G. (1990) The signal peptide. *J. Mem. Biol.*, **115**, 195–201.
58. Halic,M. and Beckmann,R. (2005) The signal recognition particle and its interactions during protein targeting. *Curr. Opin. Struct. Biol.*, **15**, 116–125.
59. Mokranjac,D. and Neupert,W. (2005) Protein import into mitochondria. *Biochem. Soc. Transac.*, **33**, 1019–1023.
60. Perocchi,F., Jensen,L., Gagneur,J., Ahting,U., von Mering,C., Bork,P., Prokisch,H. and Steinmetz,L. (2006) Assessing systems properties of yeast mitochondria through an interaction map of the organelle. *PLoS Genet.*, **2**, e170.
61. Pagliarini,D.J., Calvo,S.E., Chang,B., Sheth,S.A., Vafai,S.B., Ong,S.E., Walford,G.A., Sugiana,C., Boneh,A., Chen,W.K. *et al.* (2008) A mitochondrial protein compendium elucidates complex I disease biology. *Cell*, **134**, 112–123.
62. Hashimi,H., Cicova,Z., Novotna,L., Wen,Y.Z. and Lukes,J. (2009) Kinetoplastid guide RNA biogenesis is dependent on subunits of the mitochondrial RNA binding complex 1 and mitochondrial RNA polymerase. *RNA*, **15**, 588–599.
63. Nilsson,D., Gunasekera,K., Mani,J., Osteras,M., Farinelli,L., Baerlocher,L., Roditi,I. and Ochsenreiter,T. (2010) Spliced leader trapping reveals widespread alternative splicing patterns in the highly dynamic transcriptome of *Trypanosoma brucei*. *PLoS Path.* (In press).
64. Priest,J. and Hajduk,S. (1994) Developmental regulation of *Trypanosoma brucei* cytochrome c reductase during bloodstream to procyclic differentiation. *Mol. Biochem. Parasitol.*, **65**, 291–304.
65. Bochud-Allemann,N. and Schneider,A. (2002) Mitochondrial substrate level phosphorylation is essential for growth of procyclic *Trypanosoma brucei*. *J. Biol. Chem.*, **277**, 32849–32854.
66. Huang,L.J., Wang,L., Ma,Y., Durick,K., Perkins,G., Deerinck,T.J., Ellisman,M.H. and Taylor,S.S. (1999) NH₂-Terminal targeting motifs direct dual specificity A-kinase-anchoring protein 1 (D-AKAP1) to either mitochondria or endoplasmic reticulum. *J. Cell. Biol.*, **145**, 951–959.